

Influence of opening and closing process of sliding door on interface airflow characteristic in operating room

Zhou, Bin; Ding, Lili; Li, Fei; Xue, Ke; Nielsen, Peter Vilhelm; Xudong, Yang

Published in:
Building and Environment

DOI (link to publication from Publisher):
[10.1016/j.buildenv.2018.08.050](https://doi.org/10.1016/j.buildenv.2018.08.050)

Creative Commons License
CC BY-NC-ND 4.0

Publication date:
2018

Document Version
Accepted author manuscript, peer reviewed version

[Link to publication from Aalborg University](#)

Citation for published version (APA):
Zhou, B., Ding, L., Li, F., Xue, K., Nielsen, P. V., & Xudong, Y. (2018). Influence of opening and closing process of sliding door on interface airflow characteristic in operating room. *Building and Environment*, 144(October), 459-473. <https://doi.org/10.1016/j.buildenv.2018.08.050>

General rights

Copyright and moral rights for the publications made accessible in the public portal are retained by the authors and/or other copyright owners and it is a condition of accessing publications that users recognise and abide by the legal requirements associated with these rights.

- Users may download and print one copy of any publication from the public portal for the purpose of private study or research.
- You may not further distribute the material or use it for any profit-making activity or commercial gain
- You may freely distribute the URL identifying the publication in the public portal -

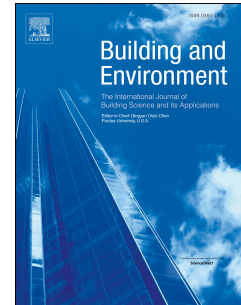
Take down policy

If you believe that this document breaches copyright please contact us at vbn@aub.aau.dk providing details, and we will remove access to the work immediately and investigate your claim.

Accepted Manuscript

Influence of opening and closing process of sliding door on interface airflow characteristic in operating room

Bin Zhou, Lili Ding, Fei Li, Ke Xue, Peter V. Nielsen, Yang Xu



PII: S0360-1323(18)30524-9

DOI: [10.1016/j.buildenv.2018.08.050](https://doi.org/10.1016/j.buildenv.2018.08.050)

Reference: BAE 5663

To appear in: *Building and Environment*

Received Date: 23 June 2018

Revised Date: 3 August 2018

Accepted Date: 24 August 2018

Please cite this article as: Zhou B, Ding L, Li F, Xue K, Nielsen PV, Xu Y, Influence of opening and closing process of sliding door on interface airflow characteristic in operating room, *Building and Environment* (2018), doi: 10.1016/j.buildenv.2018.08.050.

This is a PDF file of an unedited manuscript that has been accepted for publication. As a service to our customers we are providing this early version of the manuscript. The manuscript will undergo copyediting, typesetting, and review of the resulting proof before it is published in its final form. Please note that during the production process errors may be discovered which could affect the content, and all legal disclaimers that apply to the journal pertain.

Influence of opening and closing process of sliding door on interface airflow characteristic in operating room

Bin Zhou ^{1,*}, Lili Ding ¹, Fei Li ¹, Ke Xue ¹, Peter V. Nielsen ², Yang Xu ¹

¹ *Department of HVAC, College of Urban Construction, Nanjing Tech University, P.O. Box 76, No.*

200 North Zhongshan Rd., 210009 Nanjing, China

² *Department of Civil Engineering, Aalborg University, Aalborg, Denmark*

ABSTRACT

Indoor air environment inside operating room (OR) is crucial for the success of surgical operation. The opening and closing process of sliding door is very common in OR. In this case, the designed positive pressure will disappear. Since the air exchange characteristic at the interface of the sliding door will influence the Surgical Site Infection risk, the combined effects of temperature and pressure differences on interface airflow along with the air infiltration volume and intruding particles caused by the airflow are studied by theoretical and numerical methods. Two different cases are compared, where the temperature of OR is lower or higher than that of anteroom, respectively. Results show that the contaminants accumulate in the upper space of the OR due to the airflow pattern between two rooms when the temperature of OR is lower than the anteroom. This will increase the possibility that airflow carrying contaminants intrudes into OR. On the contrary, the contaminants are controlled in the lower space of the OR when the temperature of OR is higher than that of anteroom. On average, the particle intrusion ratio of the second case decreases by 55% compared with that of the first case. So, it is helpful to protect the clean environment of OR when the temperature of OR is higher than that of the anteroom. Moreover, the air infiltration volume of the closing phase is found unequal to that of the opening phase. This study provides the useful information for maintaining a clean indoor environment under operational condition.

Keywords: clean operating room, temperature difference, pressure difference, airborne particle, sliding door, numerical simulation

1. Introduction

Operating room is a special area for surgical treatment and rescue of patients. The air cleanliness level in this area should be maintained to reduce both the incidence of Surgical Site Infections (SSIs) and the harmful effect on patients' healthy. SSIs are common surgical complications in hospital. There are about 160,000–300,000 cases of SSIs occurring each year in America ^[1]. According to the survey data of infections in 183 American hospitals, SSIs account for 21.8% of Healthcare-Associated Infections, which is the same as the infectious rate of pneumonia ^[2]. In Europe, the incidence of SSIs also ranks the second place within HAIs ^[3], and the incidence may be higher in developing countries ^[4]. Compared with the uninfected surgical patients, the mortality rate of the patients with SSIs will increase by 2-11 times ^[5]. Besides, the hospitalization days will be prolonged and the medical expenses will thus be increased, resulting in appreciably direct and indirect economic losses.

The incidence of SSIs varies with the type of operation, the surgical technique and the patient's own immune condition. The strategies of reducing the risk of SSIs mainly focus on three aspects: patients, surgical techniques and operating environment. Air transmission is one of the most important ways leading to microbial infection of incisions. There is a correlation between SSIs and the bacterial concentration in operating room ^[6-7]. Air cleaning technologies, such as dilution with ventilation, unidirectional air distribution, pressure control and air filtration, are usually adopted to create a clean surgical environment for operating room. Based on the theoretical background for the unidirectional air distribution system ^[8], the ceiling air supply and the lower-side air return scheme is applied in most of the current operating rooms in China. The operating room maintains a certain positive pressure relative to the surrounding environment by reasonable control of supply air volume, return air volume and exhaust air volume. It is expected to prevent contaminants infiltrating into the operating room through gaps and to maintain a high air cleanliness level ^[9].

According to relevant recent investigations, due to the flow of patrol nurses and the transfer of medical equipments between operating rooms, opening and closing of the door is a very common phenomenon during the operation process ^[10-11]. However, positive pressure between operating room and adjacent room disappears shortly ^[8], and corresponding outflow will be

formed during the opening and closing of the door. Opening the door leads to the destruction of the isolation performance. And this will result in the transmission of contaminated air into the operating room^[12]. Moreover, the temperature difference will cause convection at the doorway when there is a temperature difference between two adjacent rooms^[13]. However, the convection caused by temperature difference is usually neglected in most of the previous studies. It is a concern that whether the supply airflow pattern in operating room can effectively prevent the intrusion of contaminants when there is a temperature difference.

Corresponding statistical studies found that the door opening during surgery will affect the clean indoor air quality of the operating room^[14-15]. There is a positive correlation between the times of door opening and closing and the concentration of Colony-Forming Units inside the operating room during the operative period^[10-11,16]. Each opening of the door will cause the increasing of the airborne bacterial concentration inside the operating room^[17]. Moreover, in an adjacent two-room isothermal condition, the sliding door causes less air exchange than the hinged door. However, when there is a temperature difference between the two rooms and the temperature difference increases, the air exchange rate caused by the opening and closing of the sliding door is larger^[18]. The study has shown that the incidence of SSIs can be reduced after a series of interventions (reducing the times of opening of the door)^[19]. Why does the opening and closing of the door increase the concentration of contaminants in the operating room? The answer can not be given only by methods based on statistical analysis. With the development of numerical simulation technology, it is necessary to investigate the variation characteristics of the airflow patterns at the interface of the sliding door between the operating room and the adjacent room. Therefore, the airflow exchange patterns as well as the migration and the diffusion of contaminants between the operating room and the anteroom under the effects of temperature and pressure differences will be studied numerically. Theoretical model with this combined effect will be established, and then it will be used for validation of the numerical results.

2. Theoretical analysis

Because of the different parameters such as cooling load, temperature, relative humidity, air cleanliness level and air exchange rate, different air conditioning systems will be used in the operating room and its adjacent anteroom so that the corresponding temperature difference will be

formed between them. Air convection between the two rooms will occur due to the temperature difference. The temperatures of the operating room and the anteroom can be labeled as T_n and T_w , respectively. When T_n is lower than T_w , the schematic diagram of air convection between the two rooms is shown in Fig. 1. There is a neutral plane at the center of the door height. The air exchange volume between the operating room and the anteroom is equal.

Fig. 1. Schematic diagram for airflow exchange between operating room and anteroom with temperature difference only

However, when the combined effect of temperature difference and pressure difference is considered, the schematic diagram of the airflow pattern formed at the interface of the doorway is presented in Fig.2 when the door is opened. T_n is supposed to be lower than T_w . The airflow velocity caused by positive pressure is V_x , while the presence of airflow by positive pressure will cause the neutral plane to move up.

Fig. 2. Schematic diagram of airflow exchange between operating room and anteroom with comprehensive effect of temperature difference and pressure difference

The pressures of the operating room and the anteroom at the middle height section of the doorway are P_{cn} and P_{cw} , respectively. At the section with height Z above the central line, the pressures in the operating room and the anteroom are P_n and P_w , respectively. They can be expressed as:

$$P_n = P_{cn} - \rho_n g z \quad (1)$$

$$P_w = P_{cw} - \rho_w g z \quad (2)$$

The pressure difference between the two rooms at the central line section is the same as that formed with the airflow caused by positive pressure in the operating room.

$$P_{cn} - P_{cw} = P_x \quad (3)$$

The pressure difference between the two rooms at the same level is:

$$\Delta P = P_w - P_n = (\rho_n - \rho_w) g z - P_x \quad (4)$$

Assuming that the air is the ideal gas, the air velocity caused by pressure difference at section Z according to the theory of flow dynamics can be expressed as:

$$v = \sqrt{\frac{2\Delta P}{\bar{\rho}}} = \sqrt{2g \frac{\Delta \rho}{\bar{\rho}} z} \quad (5)$$

The leakage inflow Q_{in} by positive pressure can be expressed with Eq.(6).

$$Q_{in} = C \int_{\frac{\rho V_x^2}{2\Delta \rho g}}^{\frac{H}{2}} W \left(2g \frac{\Delta \rho}{\bar{\rho}} z - V_x^2 \right)^{1/2} \cdot dz \quad (6)$$

By integrating this expression, the leakage inflow through the doorway will be:

$$Q_{in} = \frac{CW}{3} \cdot \frac{\bar{\rho}}{g\Delta \rho} \left(g \frac{\Delta \rho}{\bar{\rho}} H - V_x^2 \right)^{3/2} \quad (7)$$

In the same way, the outflow through the doorway interface will be:

$$Q_{out} = \frac{CW}{3} \cdot \frac{\bar{\rho}}{g\Delta \rho} \left(g \frac{\Delta \rho}{\bar{\rho}} H + V_x^2 \right)^{3/2} \quad (8)$$

where C is the coefficient with the value 0.5; W is width of the doorway; H is height of the doorway; g is the gravity acceleration; $\Delta \rho$ is the density difference of air in the two rooms; $\bar{\rho}$ and the mean density of air in the two rooms.

3. Numerical simulation

3.1. Physical model

As shown in Fig. 3, the physical model is established according to the size of the operating room laboratory in Nanjing. The whole model is divided into two parts, which includes the operating room and the anteroom. The dimensions of the operating room and the anteroom are 7.80 m (L) \times 5.80 m (W) \times 3.00 m (H) and 3.00 m (L) \times 6.83 m (W) \times 2.60 m (H), respectively. The operating room is separated from the anteroom through the partition wall, and the thickness of the partition wall is 0.30 m (L). A sliding door is placed in the middle of the partition wall, whose dimension is 2.00 m (W) \times 1.40 m (H). The unidirectional airflow supply opening is set at the center of the ceiling of the operating room, whose dimension is 2.60 m (L) \times 2.40 m (W). An exhaust vent is placed near the supply opening, whose dimension is 0.32 m (L) \times 0.32 m (W). There is a return vent with the dimension of 4.80 m (L) \times 0.32 m (W) on each side wall. This study focuses on the mechanism of invasion and diffusion of contaminants from the anteroom into the operating room, so the layout of the operating room under at-rest condition is adopted. There are only operating lamps and operating table inside the operating room. Both of them are located directly below the unidirectional airflow supply area, which will have a great impact on the airflow pattern. The dimension of the operating table is 1.80 m (L) \times 0.60 m (W), and the surface

of the operating table is 1.1 m above the floor. The operating lamps are simplified as cylinders with diameter of 0.40 m and thickness of 0.15 m. In the anteroom, there is an air supply opening with size of 0.70 m (L) \times 0.70 m (W) as well as an air return opening with size of 0.52 m (L) \times 0.52 m (W) on the ceiling of the anteroom.

Fig. 3. Layout of both operating room and anteroom

3.2. Governing equation

3.2.1. Turbulent airflow model

There are usually three methods for indoor airflow simulation, including DNS (Direct Numerical Simulation), LES (Large Eddy Simulation) and RANS (Reynolds-Averaged Navier-Stokes) methods. The use of DNS and LES simulation requires both large memory and fast calculation for computers. However, the RANS simulation is the most common and effective method for indoor airflow. So, both the RANS model and the standard k - ε model are adopted and compared in this study. Although the RNG k - ε model could be slightly better than the standard k - ε model and is therefore recommended for simulations of ordinary indoor airflow ^[20], it has been proved that the standard k - ε model can also be effective to predict the flow field within operating room ^[21]. The governing equation of standard k - ε model can be expressed as:

$$\frac{\partial(\rho\phi)}{\partial t} + \nabla \cdot (\rho\phi\vec{V}) = \nabla \cdot (\Gamma_\phi \nabla \phi) + S_\phi \quad (9)$$

where ∇ is the gradient of the variable; \vec{V} is the time-averaged velocity; ϕ represents each of the three velocity components (u , v , w); Γ_ϕ is the effective diffusion coefficient for each dependent variable; and S_ϕ is the source term.

3.2.2. Particle tracking model

In order to track the trajectories of the particles, the Lagrangian discrete tracking model is adopted to calculate the concentration and distribution of particles. The particle motion can be described as:

$$\frac{du_p}{dt} = F_D(u - u_p) + \frac{g(\rho_p - \rho)}{\rho_p} + F_e \quad (10)$$

where u_p is velocity of the particle; u is the velocity of the air; $F_D(u - u_p)$ is the drag force per unit particle mass; ρ_p and ρ are the particle and air densities, respectively; g is the gravitational acceleration, and F_e represents the additional forces.

The drag force follows the Stokes' law, which can be expressed as:

$$F_{\text{drag}} = F_D(u - u_p) = \frac{18\mu_a}{\rho_p d_p^2 C_c} (u - u_p) \quad (11)$$

where μ_a is fluid viscosity, d_p is particle diameter and C_c is Cunningham correction factor.

The third term on the right side of Eq. (10) represents the other forces such as the pressure gradient force, Brownian force, thermophoretic force and Saffman's lift force, *etc.* Based on the simulation and experimental results of Chang and Hu, the Saffman's lift force has a great impact on particles with size in the range of 2.5 to 5 μm , while Brownian force has larger effect on particles with size less than 0.5 μm [22]. Therefore, the influence of Brownian force is ignored, and the effects of Saffman's lift force, pressure gradient force and thermophoretic force are considered only in this study. In addition, considering the influence of turbulence on the particle diffusion, the discrete random walk model (DRW) is used in order to obtain the diffusion of particles with turbulence pulsation.

3.2.3. Dynamic mesh model

In order to realize the opening and closing process of the door, dynamic mesh model is adopted. The integral form of the conservation equation for a general scalar ϕ , on an arbitrary control volume whose boundary is moving, can be expressed as:

$$\frac{d}{dt} \int_V \rho \phi dV + \int_{\partial V} \rho \phi (\vec{u} - \vec{u}_g) \cdot d\vec{A} = \int_{\partial V} \Gamma \nabla \phi \cdot d\vec{A} + \int_V S_\phi dV \quad (12)$$

where ρ is the fluid density, \vec{u} is the flow velocity vector, \vec{u}_g is the mesh velocity of the moving mesh, Γ is the diffusion coefficient, S_ϕ is the source term, and ∂V is the boundary of the control volume.

The finite volume method (FVM) is applied to transform the above-mentioned differential equations into the discrete equations. Second-order upwind schemes are adopted for differential derivatives. A Semi-Implicit Method for Pressure-Linked Equations (SIMPLE) algorithm is used

while discretized equations for each variable is solved by Gauss-Seidel iteration scheme. The convergence criteria are set as follows: the residuals for both the velocity in the directions of X, Y and Z and the continuity reached 10^{-4} , and the energy residual reached 10^{-6} .

3.3. Boundary conditions

The unidirectional airflow supply opening is defined as the boundary of velocity inlet. A suitable air velocity should be formed when the air-supply decreases near the working area of the operating table. The "Architectural Technical Code for Hospital Clean Operating Department" stipulates that the average air velocity in the working area should be 0.20-0.25 m/s. When the air supply velocity is set at 0.45 m/s, this regulation can be satisfied, and the corresponding air supply air volume in operating room is 10108 m³/h. The air return opening and the exhaust vent in operating room are both defined as the boundary of velocity outlet. The supply air velocity in the anteroom is 0.25 m/s, and the boundary type of the air return opening in anteroom is defined as outflow. The positive pressure difference is formed between the operating room and the anteroom through the difference among the air supply volume, the air return volume and the air exhaust volume. The outdoor air volume of operating room is 810 m³/h and the exhaust air volume is 360 m³/h, so the differential air volume to form positive pressure is 450 m³/h. The gap is 0.006 m, and the positive pressure of 6 Pa can be maintained between the operating room and the anteroom, which corresponds to 450 m³/h positive pressure air volume when the door is closed. The time for the whole process of door opening and closing is 18 s. From 0 s to 7 s, it is the opening phase of the door. From 7 s to 11 s, the door is kept in full opened state. From 11 s to 18 s, it is the closing phase of the door. The specific types and values of the boundary conditions are shown in Table 1. The temperature in operating room should be between 21°C and 25°C according to corresponding literature^[23]. In this study, it is found that when the temperature of the supply air is set as 23°C, the temperature in the operating room can meet the requirement of standard.

Table 1 Model information and parameter values of boundary condition

Persons are the main sources of particles in the anteroom. Meanwhile, the floor, the surrounding walls and the ceiling will also generate particles. According to relevant literature ^[8], the particle quantity generated by a still person is 1×10^5 CFU/min. The particle quantity generated by a person is 5×10^5 CFU/min when he is in an active movement condition. Moreover, the particle quantity generated by surfaces of enclosure structure is based on the floor. The quantity of particles released by 8 square meters of floor is about the same as that of a still person. So the particle quantity generated by the floor and the surfaces of enclosure structure is 1.25×10^4 CFU/(min·m²). It is assumed that there is one person in activity in the anteroom, and the total quantity of particles generated by the anteroom environment is 18100 CFU/s. The sedimentation and resuspension effect of particles are neglected. The particles generated by the anteroom are simplified. It is assumed that the particles will uniformly distribute in the anteroom. Particles are released for 30 seconds before opening the door, and a relatively uniformly-distributed initial particle concentration field will be formed in the anteroom.

The sources of particles in the anteroom are complex and the particle sizes are quite different. Breathing, coughing and sneezing of person can generate droplets. It is found that the droplets sizes generated by coughing behavior range from 1.1 to 3.3 μm through Anderson sampler measurements ^[24]. There will be a large number of particles released from the surface of clothing when person is in activity. It is found that the size of the particles from the surface of clothing are more concentrated between 3 to 10 μm when a person wearing cleanroom clothing is in activity through experimental study ^[25]. Different sizes including 1 μm , 3 μm , 5 μm and 7 μm were calculated. It is found that only marginal difference was found among the results, so the diameter of 5 μm is selected for the following calculation.

3.4. Hypothesis of the model

Under the premise of ensuring the accuracy of the calculation results, the following assumptions are made for the model:

- (1) Indoor air is incompressible ideal gas;
- (2) Radiation heat transfer is simplified. The only heat sources in the operating room are operating lamps which are set as constant heat flux boundary. The radiation heat of the operating

lamps will go through the surfaces of the lamps, which releases heat to the operating room ^[26].

(3) All walls and operating table surfaces are set to be adiabatic boundaries.

(4) Initial uniform temperature field is formed in both operating room and anteroom, and the temperature stratification is not taken into consideration.

3.5. Layout of monitoring points

The volume of air exchange between the operating room and the anteroom is calculated according to the method of corresponding literature ^[27]. The location of the monitoring points for air velocity at the doorway interface is shown in Fig.4. The calculation process of airflow volume is as follows:

(1) Recording the air velocity V_x in the X direction at the monitoring points.

(2) The area of the doorway is discretized according to the location of the monitoring points and divided into several small regions. The airflow volume in each small region is the product of the air velocity V_x and the area of this region.

(a) Schematics of monitoring point

(b) Location of monitoring point

Fig. 4. Layout of monitoring points at the interface for measuring air velocity

At the same time, in order to monitor and calculate the variation of pressure difference between two rooms with time, the pressure monitoring points were placed in the operating room and anteroom apart, which are 0.4 m inwards and outwards from C1, C2, C3, C4 and C5 points, respectively.

3.6. Grid independence test

The grid independence test is carried out on the model. Numerical simulations are performed with the mesh numbers of 381254, 458216, 623579, 732451, 982536 and 1176284, respectively. It is shown in Fig. 5 that when the mesh number is equal to and larger than 732451, the air velocity at the center of the projection area of the unidirectional air supply outlet at $Y=1.2\text{m}$ reaches stable.

Therefore, the grid number of 732451 was chosen in the following simulation.

Fig. 5. Air velocity at the center of the projection area of the unidirectional air supply outlet at
Y=1.2m

3.7. Simulation conditions

The first case is described as follows. A uniform temperature field at 23°C is formed on the basis of the unidirectional supply air temperature in the operating room. Different temperature fields in the front chamber are formed by setting different supply air temperatures, thus forming conditions of different temperature differences. The temperature of the operating room is lower than that of the anteroom ($T_n < T_w$) under this case. Specific condition setting is shown in Table 2.

Table 2 Settings of temperature difference between operating room and anteroom ($T_n < T_w$)

The method of forming conditions of different temperatures under the second case is the same as the above. However, the temperature of the operating room is higher than that of the anteroom ($T_n > T_w$) under this case. Specific condition of setting is shown in Table 3.

Table 3 Setting of temperature difference between operating room and anteroom ($T_n > T_w$)

3.8. Particle intrusion assessment index

In order to analyze the migration and dispersion of particles from the anteroom into the operating room as well as assess the severity of the intrusion of particles, and the coefficient of particle intrusion ratio K is defined as:

$$K = \frac{M_i}{M} \quad (13)$$

where M_i is the quantity of particles intrude into operating room during the opening and closing

process of the door; M is the total quantity of particles in the anteroom before the opening of the door.

4 Results and discussion

4.1. Validation of mathematical model

In order to validate the mathematical model in this study, the measurement data of airflow distribution on the full-scale ISO Class-5 cleanroom in a hospital by Yang *et al.* were used^[28]. The experimental data in corresponding literature^[29] were used to verify the reliability of the Lagrangian discrete tracking model. The validation of the numerical method can be found in Appendix A as the online supplementary material.

The simulated flow field and particle trajectory agree well with the measured values. It is verified that the standard k - ε model is reliable and can be selected for the numerical simulation in the following study. Moreover, when the experimental data by Kalliomaki *et al.*^[12] is used, it is also proved that this model can be applied to obtain the air exchange rate between two adjacent rooms with sliding door.

4.2. Variety of pressure difference between two rooms

The variation of pressure difference with opening and closing process of the door under condition 2-3 is shown in Fig. 6. The temperature in the operating room is higher than that in the anteroom under this condition, and the temperature difference is 3°C. It can be found that variations of pressure difference at difference positions have the same trends, where the pressure difference drops sharply with the opening of the door. At the time of 1s after opening of the door, the pressure difference is almost 0. However, the pressure difference reappears after the closing of the door. Besides, the pressure in the operating room is slightly higher than that in the anteroom at the upper part of the doorway such as the position of A₄, A₅, C₄, C₅, E₄ and E₅. This is due to the thermal pressure caused by temperature difference. On the contrary, the pressure in the operating room is slightly lower than that in the anteroom at the lower part of the doorway.

(a) Position A₁ to A₅(b) Position C₁ to C₅(c) Position E₁ to E₅

Fig. 6. Variation of pressure difference with opening and closing process of the door under condition 2-3

4.3. Analysis of airflow exchange and particles intrusion between two rooms under case 1

4.3.1. Analysis of airflow exchange between two rooms

When the temperature in the operating room is lower than that in the anteroom, the airflow exchange pattern and temperature distribution between the operating room and the anteroom are shown in Fig. 7. Since $t=11s$ is the last moment of the full opened phase of the door, the air exchange between the operating room and the anteroom is the most intensive. So the simulation results of $t=11s$ are selected in the following analysis. The detailed analysis is carried out with the condition 1-1 as an example. The velocity vector diagram in $Z=3.4m$ plane under condition 1-1 is shown in Fig. 7(I-b). The warmer air in the anteroom encounters with the colder air in the operating room at the doorway interface. Thus, the warmer air rises and the colder air sinks, forming a typical natural convection caused by temperature difference, where the air flows from the operating room to the anteroom through the lower part of the doorway and the air flows from the anteroom to the operating room through the upper part of the doorway. As shown in Fig. 7(I-b), the convection by temperature difference and outflow by positive pressure are superimposed, which enhances airflow exchange between two rooms. This airflow pattern forms a vortex near the doorway, which will carry particles of the anteroom into the operating room. From Fig. 7(I-b) to Fig. 7(V-b), it is shown that with the increase of temperature difference, the airflow exchange between the two rooms becomes more intensive, and the range of the vortex is also expanded.

(I) Condition 1-1, $\Delta T=1^{\circ}C$, $t=11s$

(II) Condition 1-2, $\Delta T=2^{\circ}C$, $t=11s$

(III) Condition 1-3, $\Delta T=3^{\circ}\text{C}$, $t=11\text{s}$

(IV) Condition 1-4, $\Delta T=4^{\circ}\text{C}$, $t=11\text{s}$

(V) Condition 1-5, $\Delta T=5^{\circ}\text{C}$, $t=11\text{s}$

(a) Temperature contour in plane $Z=3.4\text{m}$

(b) Velocity vector in plane $Z=3.4\text{m}$

Fig. 7. Contour of temperature and velocity vector under condition 1-1 ~ 1-5 when $T_n < T_w$

Fig. 8 illustrates the air infiltration rate from anteroom into operating room with time under conditions 1-1 to 1-5 during the opening and closing process of the door. It is obvious that the infiltration air volume increases with the increase of temperature difference. The infiltration air volume is almost 0 in the first 2 seconds under each condition, and there exist infiltration airflow after 2 seconds. This is due to the constant outflow volume by positive pressure from the operating room. With the increasing of the opening area of the door, the corresponding velocity of outflow by positive pressure reduces. In the first 2 seconds, the opening area of the door is small, and the effect of temperature difference is weak due to the small contact surface of the air between the two rooms. Therefore, outflow by positive pressure completely counteracts that by temperature difference during this period. After 2 seconds, the effect of temperature difference appears, and the velocity of outflow by positive pressure decreases gradually. In this case, it can't completely counteract the effect of temperature difference. The variation trend of infiltration air volume under each condition is essentially the same. Therefore, the airflow pattern at the doorway interface is displayed by taking the results of condition 1-3 as an example. The velocity vector diagram at the doorway interface when the temperature difference is 3°C is shown in Fig. 9. All the air flows from the operating room to the anteroom at the interface of the doorway in the first 2 seconds. With the increasing of the opening area of the door, airflow will infiltrate into the operating room from the anteroom through the upper part of the doorway. The air infiltration rate increases with the opening area of the door. Moreover, the airflow pattern at the doorway interface is displayed in Fig. 10 by taking the results of condition 2-3 with the temperature difference 3°C . In the first 2 seconds, all the air flows from the operating room to the anteroom. When the opening area of the sliding door increases, airflow will infiltrate into the operating room from the anteroom through the lower part of the doorway.

Fig. 8. Air infiltration rates from anteroom into operating room under condition 1-1~1-5

- (a) Opening of the door $\Delta Z=0.4\text{m}$, $t=2\text{s}$ (b) Opening of the door $\Delta Z=0.8\text{m}$, $t=4\text{s}$
 (c) Opening of the door $\Delta Z=1.2\text{m}$, $t=6\text{s}$ (d) Opening of the door $\Delta Z=1.4\text{m}$, $t=8\text{s}$

Fig. 9. Variation of velocity vector at the interface with door opening under condition 1-3

- (a) Opening of the door $\Delta Z=0.4\text{m}$, $t=2\text{s}$ (b) Opening of the door $\Delta Z=0.8\text{m}$, $t=4\text{s}$
 (c) Opening of the door $\Delta Z=1.2\text{m}$, $t=6\text{s}$ (d) Opening of the door $\Delta Z=1.4\text{m}$, $t=8\text{s}$

Fig. 10. Variation of velocity vector at the interface with door opening under condition 2-3

The effect of temperature difference enhances the air exchange rate between two rooms through the whole opening and closing process of the door. As shown in Fig. 9 and Fig. 11, the air infiltration volume of the closing phase is much larger than that of the opening phase. From condition 1-1 to 1-5, the air infiltration volume of the closing phase is about 3 times that of the opening phase on average. The opening phase of door and the closing phase of door are symmetrical to the full opening phase. But the air infiltration volumes of the two phases are quite different. This is attributed to the balance between the positive pressure effect and the temperature difference effect. When the door is kept at the full opened state, the temperature difference effect reaches the maximum while the positive pressure effect reaches the minimum. Moreover, this is also attributing to the inertia of the airflow exchanged between two rooms. Therefore, the air infiltration volumes during the opening and closing process of the door are different.

Fig. 11. The infiltration air volume at different phases under condition 1-1~1-5 when $T_n < T_w$

4.3.2. Analysis of particles intrusion between two rooms

The particle concentration contours in plane $Y=1.2\text{m}$ and $Z=3.4\text{m}$ at the time of 11 seconds under conditions 1-1 to 1-5 are shown in Fig. 12. From Fig. 12(I-a) to 12(V-a), it is shown that the distribution of particles with height and the approximate degree of intrusion of particles. It is obvious that particles spread into the operating room with the airflow and accumulate in the upper space of the operating room near the doorway. Both the amount of intruding particles and the depth of intrusion increase with the increase of temperature difference. The particle concentration contours in plane $Y=1.2\text{m}$ are shown in Fig. 12(I-b) to 12(V-b). Since $Y=1.2\text{m}$ is the height corresponding to the surgical area, the particle distribution in plane $Y=1.2\text{m}$ are selected for analysis. It can be seen from the contours that the particle concentration at the height of $Y=1.2\text{m}$ is very small under all conditions, and the particles are mostly distributed above the height of $Y=1.2\text{m}$. Although the particle concentration in the plane of surgical area is very small, these particles accumulate in the upper space of the operating room, which is contrary to the concept of environmental control in operating room. The ceiling air supply and lower-side air return scheme is used in operating room. This is because the contaminants can be controlled in the lower space of the operating room and be quickly discharged. The medical staffs are neglected in the simulation of this paper. However, there will be frequent personnel activities to disrupt the stable airflow distribution and to destroy the protective effect of the mainstream air supply for the surgical area. Thus, the accumulation of particulate matter in the upper space of the operating room may cause a potential threat to the surgical area.

(I) Condition 1-1, $\Delta T=1^\circ\text{C}$, $t=11\text{s}$

(II) Condition 1-2, $\Delta T=2^\circ\text{C}$, $t=11\text{s}$

(III) Condition 1-3, $\Delta T=3^\circ\text{C}$, $t=11\text{s}$

(IV) Condition 1-4, $\Delta T=4^{\circ}\text{C}$, $t=11\text{s}$

(V) Condition 1-5, $\Delta T=5^{\circ}\text{C}$, $t=11\text{s}$

(a) Particle concentration contour in plane $Z=3.4\text{m}$ (b) Particle concentration contour in plane $Y=1.2\text{m}$

Fig. 12. Contour of particle concentration under condition 1-1~1-5 when $T_n < T_w$

4.4. Analysis of airflow exchange and particles intrusion between two rooms under case 2

4.4.1. Analysis of airflow exchange between two rooms

When the temperature in the operating room is higher than that in the anteroom, the airflow exchange pattern and temperature distribution between the operating room and the anteroom are shown in Fig. 13. The velocity vector maps in plane $Z=3.4\text{m}$ at the time of 11 seconds under condition 2-1 to condition 2-5 are shown in Fig. 13(I-b) to Fig. 13(V-b), respectively. The following example is illustrated in Fig. 13(I-b) with a temperature difference of 1°C . Under the effect of temperature difference, the air flows from the anteroom to the operating room through the lower part of the doorway, but the supply airflow in the operating room is just opposite to this airflow. So, it's different from the above first case that the convection by temperature difference and outflow by positive pressure are no longer superimposed but counteract with each other, when the temperature in the operating room is higher than that in the anteroom. The colder air in the anteroom encounters with the warmer air in the operating room at the doorway interface, and the warmer air flows upward to form the outflow at the upper part of the doorway. From Fig. 13(I-b) to Fig. 13(V-b), the outflow through the upper part of the doorway is more intensive with the increasing of the temperature difference.

(I) Condition 2-1, $\Delta T=1^{\circ}\text{C}$, $t=11\text{s}$

(II) Condition 2-2, $\Delta T=2^{\circ}\text{C}$, $t=11\text{s}$

(III) Condition 2-3, $\Delta T=3^{\circ}\text{C}$, $t=11\text{s}$

(IV) Condition 2-4, $\Delta T=4^{\circ}\text{C}$, $t=11\text{s}$

(V) Condition 2-5, $\Delta T=5^{\circ}\text{C}$, $t=11\text{s}$

(a) Temperature contour map in plane $Z=3.4\text{m}$

(b) Velocity vector map in plane $Z=3.4\text{m}$

Fig. 13. Contour of temperature and velocity vector under condition 2-1~2-5 when $T_n > T_w$

Fig. 14 presents the air infiltration rate from anteroom into operating room with time under conditions 2-1 to 2-5 during the opening and closing process of the door. In the case of $T_n > T_w$, it is interesting that the air infiltration rate doesn't increase with the increase of temperature difference under condition 2-1 to 2-5, and the minimum air infiltration rate occurs when the temperature difference is 2°C . This is due to the best effect of convection by temperature difference and outflow by positive pressure counteracting with each other when the temperature difference is 2°C . As shown in Fig. 13(I-b), when the supply airflow rises upward, one part of the airflow comes into the anteroom to form an outflow, and the other part of the airflow returns to the operating room to form a backflow under condition 2-1 when the temperature difference is 1°C . However, when the temperature difference is 2°C , the supply airflow almost flows out of the operating room after rising and very few air flows back into the operating room. The outflow by positive pressure provides a barrier effect at the doorway interface, which effectively reduces the airflow from the anteroom into the operating room. The convection by temperature difference becomes more and more intensive with the increase of the temperature difference under conditions 2-3 to 2-5, so there is airflow coming into the operating room from the anteroom through the lower part of the doorway, and a "triangle" vortex zone is formed near the doorway.

Fig. 14. Air infiltration rate from anteroom into operating room under condition 2-1~2-5

Fig. 15. Volume of infiltration air at different phases under condition 2-1~2-5 when $T_n > T_w$

From Fig. 14 and Fig. 15, it can be found that the air infiltration volume of the closing phase is also much larger than that of the opening phase. On average, the air infiltration volume of the closing phase for conditions 2-1 to 2-5 is about 4.7 times that of the opening phase. This is also attributed to the inertial effect of airflow after the door is kept full-opened. But, it is different that

the air infiltration volume of the closing phase even exceeds the air infiltration volume of the full opened phase of the door under the conditions 2-3, 2-4 and 2-5. This is due to the phenomenon of convection by temperature difference and outflow by positive pressure counteracting with each other, which slows down the development of the effect of temperature difference. So the effect of temperature difference achieves the strongest during the closing phase of the door.

4.4.2. Analysis of particles intrusion between two rooms

The particle concentration contours in plane $Y=1.2\text{m}$ and $Z=3.4\text{m}$ at the time of 11 seconds under conditions 2-1 to 2-5 are shown in Fig. 16. The backflow carries a few particles into the operating room through the upper part of the doorway when the temperature difference is 1°C . The outflow by positive pressure provides a barrier effect at the doorway interface, which effectively reduces the intrusion of particles when the temperature difference is 2°C . Particles spread into the operating room with the airflow and accumulate in the "triangle" vortex zone when the temperature difference is 3°C or larger. The range of the vortex zone is larger as the temperature difference increases. In this case, the intrusion depth of the particles is only about 0.5m , and the particles are controlled in the lower space of the operating room, which is more consistent with environmental control concept of operating room. And compared with the first case ($T_n < T_w$), both the intrusion range and intrusion depth of particles are smaller.

(I) Condition 2-1, $\Delta T=1^\circ\text{C}$, $t=11\text{s}$

(II) Condition 2-2, $\Delta T=2^\circ\text{C}$, $t=11\text{s}$

(III) Condition 2-3, $\Delta T=3^\circ\text{C}$, $t=11\text{s}$

(IV) Condition 2-4, $\Delta T=4^\circ\text{C}$, $t=11\text{s}$

(V) Condition 2-5, $\Delta T=5^\circ\text{C}$, $t=11\text{s}$

(a) Particle concentration contour in plane

 $Z=3.4\text{m}$

(b) Particle concentration contour in plane

 $Y=1.2\text{m}$ **Fig. 16.** Contour of particle concentration under condition 2-1~2-5 when $T_n > T_w$

4.5. Comparison of the particle intrusion ratio under different cases

As shown in Fig. 17, the particle intrusion ratio increases with the increase of temperature difference under case 1. Under case 2, the minimum particle intrusion ratio occurs when the temperature difference is 2°C . The particle intrusion ratio increases with the increase of temperature difference when $\Delta T > 2^\circ\text{C}$ in case 2. Moreover, the particle intrusion ratio of case 2 decreased by 80% compared with that of case 1 when the temperature difference is 2°C . The average particle intrusion ratio of case 2 is smaller than that of case 1 by 55%. Therefore, it is suggested that the temperature in the operating room should be higher than that in the anteroom. The temperature difference between the operating room and the adjacent room should be controlled at 1 to 2°C , so as to achieve the best effect of reducing the amount of intrusion contaminant. Videos related to this two scenarios can be found as online supplementary materials.

Fig. 17. Comparison of particle intrusion ratios between Case 1 and Case 2

4.6. Comparison of simulated air volume and theoretical air volume

Comparison of the exchange airflow rate between two rooms under condition 2-3 calculated by Eq. (7) and Eq. (8) with the simulated value is shown in Fig. 18.

It can be found that the trends of theoretical value and simulated value with time are essentially the same. In most of the time, the error between theoretical calculation and simulated value is less than 10%. The theoretical value is larger than the simulated value, especially in the opening stage of the door. This is also attributing to the inertia of the airflow exchanged between two rooms. In theoretical calculation, the effect of temperature difference effect has reached the strongest effect from the very beginning, and it doesn't change with the opening and closing process of the door. So the theoretical calculation value is larger.

(a) Air infiltration rate into the operating room (b) Air outflow rate from the operating room

Fig. 18. Comparison of the simulated and theoretical exchange airflow rate between two rooms

4.7. Limitation

(1) Only numerical simulation and theoretical analysis have been carried out in this paper, and further experimental studies should be performed for validation.

(2) The pressure difference is constant in this study. Further study is needed about coupling effect of various pressure differences and temperature differences.

(3) The combined influence characteristic of the people flow should be investigated systematically in future study.

5. Conclusions

In summary, it is an indisputable fact that there exists temperature difference between the operating room and adjacent room. However, a reasonable control strategy for temperature difference should be adopted to prevent contaminants from intruding into operating room and to maintain a clean indoor environment. The conclusions of this study are as follows.

(1) The convection by temperature difference and outflow by positive pressure are superimposed under case 1. This will increase the possibility that airflow carrying contaminants intrudes into operating room and it is adverse to the clean environment of operating room. On the contrary, the convection by temperature difference and outflow by positive pressure counteract with each other under case 2. The outflow by positive pressure provides a barrier effect at the doorway interface, which effectively reduces the intrusion of contaminants.

(2) The depth of particles intrusion as well as the particle intrusion ratio of case 1 are larger than those of case 2. On average, the particle intrusion ratio of case 2 decreases by 55% compared with that of case 1.

(3) According to the airflow exchange and particles intrusion between two rooms in two cases, the temperature in the operating room should be higher than that in the anteroom. It is suggested that the temperature difference between the operating room and the adjacent rooms should be controlled at 1 to 2°C, so as to achieve the best effect of reducing the amount of intrusion

contaminant.

Acknowledgements

This work is financially supported by the National Natural Science Foundation of China (No. 51508267, 51708286), the Six Talent Peaks Project of Jiangsu Province (JNHB-043), the Natural Science Foundation of Jiangsu Province (No. BK20171015, BK20130946), Postgraduate Research & Practice Innovation Program of Jiangsu Province in 2018 (KYCX18_1056) and the Scientific Research Foundation from Nanjing Tech University (No. 44214122). Acknowledgement is also given to anonymous reviewers for their constructive comments.

References

- [1] Anderson DJ, Podgorny K, Berrios-Torres SI, Bratzler DW, Dellinger EP, Greene L, Nyquist AC, Saiman L, Yokoe DS, Maragakis LL, Kaye KS, Strategies to Prevent Surgical Site Infections in Acute Care Hospitals: 2014 Update, *Infect. Cont. Hosp. Ep.* 35(6) (2014) 605-627.
- [2] Magill SS, Edwards JR, Bamberg W, Beldavs ZG, Dumyati G, Kainer MA, Lynfield R, Maloney M, McAllister-Hollod L, Nadle J, Ray SM, Thompson DL, Wilson LE, Fridkin SK, Multistate point-prevalence survey of health care-associated infections. *New Engl. J. Med.* 370(13) (2014) 1198-1208.
- [3] Berrios SI, Umscheid CA, Bratzler DW, Leas B, Stone EC, Kelz RR, Reinke CE, Morgan S, Solomkin JS, Mazuski JE, Dellinger EP, Itani KMF, Berbari EF, Segreti J, Parvizi J, Blanchard J, Allen G, Kluytmans JAJW, Donlan R, Schechter WP, Centers for disease control and prevention guideline for the prevention of Surgical Site Infection, 2017. *JAMA Surg.* 152(8) (2017) 784-791.
- [4] Allegranzi B, Nejad SB, Combescure C, Graafmans W, Attar H, Donaldson L, Pittet D, Burden of endemic health-care-associated infection in developing countries: systematic review and meta-analysis, *LANCET.* 377(9761) (2011) 228-241.
- [5] Wang J, Hu J, Harbarth S, Pittet D, Zhou M, Zingg W, Burden of healthcare-associated

- infections in China: results of the 2015 point prevalence survey in Dong Guan City, *J. Hosp. Infect.* 96(2) (2017) 132-138.
- [6] Xie DS, Xiong W, Xiang LL, Fu XY, Yu YH, Liu L, Huang SQ, Wang XH, Gan XM, Xu M, Wang HB, Xiang H, Xu YH, Nie SF, Point prevalence surveys of healthcare-associated infection in 13 hospitals in Hubei Province, China, 2007-2008, *J. Hosp. Infect.* 76(2) (2010) 150-155.
- [7] Liu JY, Wu YH, Cai M, Zhou CL, Point-prevalence survey of healthcare-associated infections in Beijing, China: a survey and analysis in 2014, *J. Hosp. Infect.* 93(3) (2016) 271-279.
- [8] Xu ZL, *Fundamentals of Air Cleaning Technology and Its Application in Cleanrooms*, Berlin: Springer Press, 2014.
- [9] Sadrizadeh S, Afshari A, Karimipannah T, Håkansson U, Nielsen PV, Numerical simulation of the impact of surgeon posture on airborne particle distribution in a turbulent mixing operating theatre, *Build. Environ.* 110 (2016) 140-147.
- [10] Smith EB, Raphael IJ, Maltenfort MG, Honsawek S, Dolan K, Younkins, EA, The effect of laminar air flow and door openings on operating room contamination, *J. Arthroplasty.* 28(9) (2013) 1482-1485.
- [11] Teter J, Guajardo I, Al-Rammah T, Rosson G, Perl TM, Manahan M, Assessment of operating room airflow using air particle counts and direct observation of door openings, *AM. J. Infect. Control.* 45(5) (2017) 477-482.
- [12] Kalliomaki P, Saarinen P, Tang JW, Koskela H, Airflow patterns through single hinged and sliding doors in hospital isolation rooms - Effect of ventilation, flow differential and passage, *Build. Environ.* 107 (2016) 154-168.
- [13] Sadrizadeh S, Pantelic J, Sherman M, Clark J, Abouali O, Airborne particle dispersion to an operating room environment during sliding and hinged door opening, *J. Infect. Public Heal.* (2018) (In Press).
- [14] Wilson DJ, Kiel DE, Gravity driven counterflow through an open door in a sealed room, *Build. Environ.* 25(4) (1990) 379-388.
- [15] Tung YC, Shih YC, Hu SC, Numerical study on the dispersion of airborne contaminants from an isolation room in the case of door opening, *Appl. Therm. Eng.* 29(8-9) (2009) 1544-1551.
- [16] Andersson AE, Bergh I, Karlsson J, Eriksson BI, Nilsson K, Traffic flow in the operating

- room: An explorative and descriptive study on air quality during orthopedic trauma implant surgery, *AM. J. Infect. Control.* 40(8) (2012) 750-755.
- [17] Stauning MT, Bediako-Bowan A, Andersen LP, Opintan JA, Labi A-K, Kurtzhals JAL, Bjerrum S, Traffic flow and microbial air contamination in operating rooms at a major teaching hospital in Ghana, *J. Hosp. Infect.* DOI:10.1016/j.jhin.2017.12.010.
- [18] Lee S, Park B, Kurabuchi T, Numerical evaluation of influence of door opening on interzonal air exchange, *Build. Environ.* 102 (2016) 230-242.
- [19] Crolla RMPH, van der Laan L, Veen EJ, Hendriks Y, van Schendel C, Kluytmans, J, Reduction of Surgical Site Infections after implementation of a bundle of care, *PLOS ONE.* 7(9) (2012) e44599.
- [20] Chen Q, Comparison of different $k-\epsilon$ models for indoor airflow computations, *Numer. Heat Tr. B-Fund.* 28(3) (1995) 353-369.
- [21] Chow TT, Wang J, Dynamic simulation on impact of surgeon bending movement on bacteria-carrying particles distribution in operating theatre, *Build. Environ.* 57(3) (2012) 68-80.
- [22] Chang TJ, Hu TS, Transport mechanisms of airborne particulate matters in partitioned indoor environment, *Build. Environ.* 43(5) (2008) 886-895.
- [23] National Health and Family Planning Commission of PRC, Architectural technical code for hospital clean operating department (GB 50333-2013), Beijing: China Architecture & Building Press, 2013. (in Chinese)
- [24] Fennelly KP, Martyny JW, Fulton KE, Orme IM, Cave DM, Heifets LB, Cough-generated Aerosols of *Mycobacterium tuberculosis*: A New Method to Study Infectiousness, *AM. J. Resp. Crit. Care.* 169(5) (2004) 604-609.
- [25] Mcdonagh A, Byrne MA, A study of the size distribution of aerosol particles resuspended from clothing surfaces, *J. Aerosol. Sci.* 75(3) (2014) 94-103.
- [26] Nielsen PV, Allard F, Abwi HB, Davidson L, Schälin A, Computational Fluid Dynamics in Ventilation Design: REHVA Guidebook, No. 10, REHVA, Forssa, Finland, 2007.
- [27] Villafruela JM, San Jose JF, Castro F, Zarzuelo A, Airflow patterns through a sliding door during opening and foot traffic in operating rooms, *Build. Environ.* 109 (2016) 190-198.
- [28] Yang CQ, Yang XY, Zhao B, The ventilation needed to control thermal plume and particle

dispersion from manikins in a unidirectional ventilated protective isolation room, Build. Simul-China. 8(5) (2015) 551-565.

- [29] Lu WZ, Howarth AT, Adam N, Riffat SB, Modelling and measurement of airflow and aerosol particle distribution in a ventilated two-zone chamber, Build. Environ. 31(5) (1996) 417-423.

Table 1 Model information and parameter values of boundary condition

Model type	Dimension (m)	Boundary type	Related parameters
Operating room	$7.80 (X) \times 5.80 (Z) \times 3.00 (Y)$	Wall	Adiabatic
Anteroom	$3.00 (X) \times 6.80 (Z) \times 2.60 (Y)$	Wall	Adiabatic
Laminar airflow supply opening	$2.60 (X) \times 2.40 (Z)$	Velocity-inlet	0.45 m/s, 23°C
Air return opening in operating room	$4.80 (X) \times 0.32 (Y)$	Velocity-outlet	0.84m/s
Air exhaust opening in operating room	$0.30(X) \times 0.30(Z)$	Velocity-outlet	1.00m/s
Air supply opening in anteroom	$0.70(X) \times 0.70(Z)$	Velocity-inlet	0.25m/s
Air return opening in anteroom	$0.50(X) \times 0.50(Z)$	Outflow	—
Door	$1.50(Z) \times 2.10(Y) \times 0.05(X)$	Wall	Adiabatic
Operating lamp	Diameter: 0.40, Thickness:0.15	Wall	Heat release rate: 200W/m ²
Operating table	Table top: $1.8(X) \times 0.6(Z)$, Height:1.1	Wall	Adiabatic

Table 2 Settings of temperature difference between operation room and anteroom ($T_n < T_w$)

Conditions	1-1	1-2	1-3	1-4	1-5
T_n (°C)	24	25	26	27	28
ΔT (°C)	1	2	3	4	5

Table 3 Setting of temperature difference between operation room and anteroom ($T_n > T_w$)

Conditions	2-1	2-2	2-3	2-4	2-5
T_n (°C)	22	21	20	19	18
ΔT (°C)	1	2	3	4	5

Operating room

T_n

Anteroom

T_w

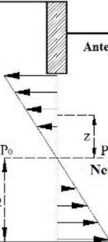
P_0

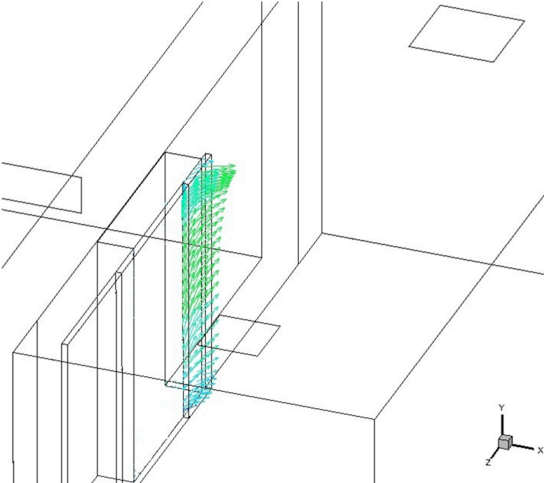
P_0

Neutral surface

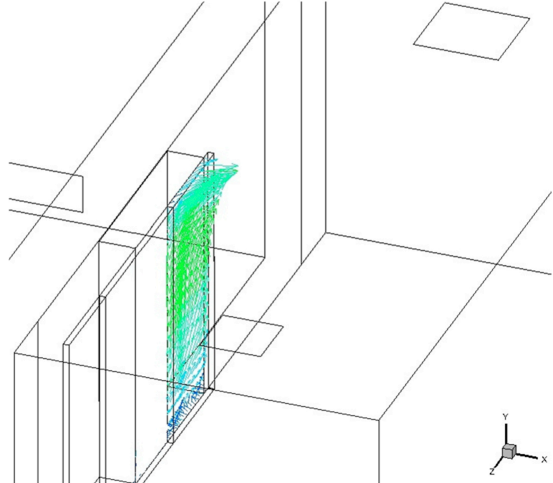
$H/2$

z

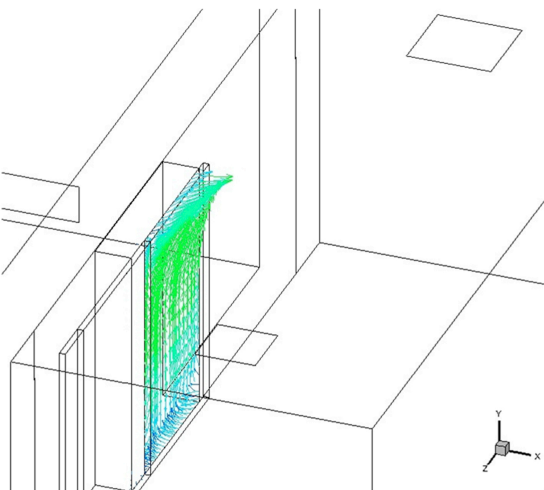




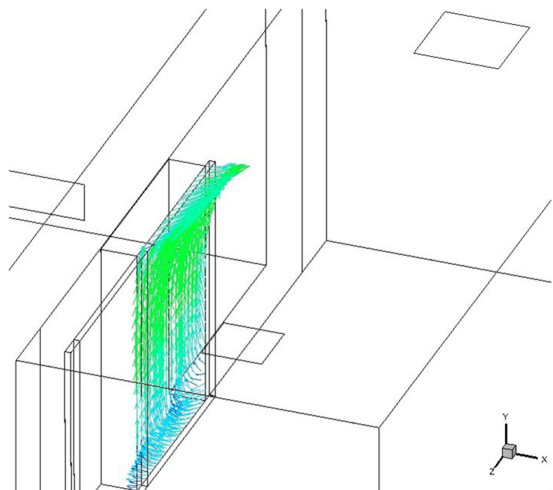
(a) Opening of the door $\Delta Z=0.4\text{m}$, $t=2\text{s}$



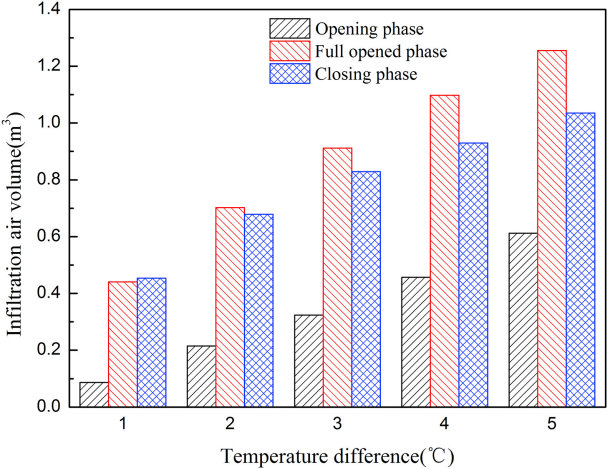
(b) Opening of the door $\Delta Z=0.8\text{m}$, $t=4\text{s}$

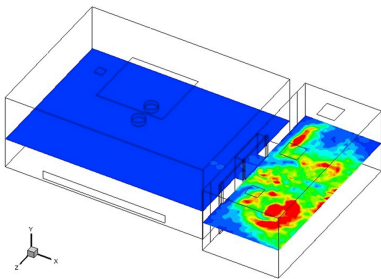
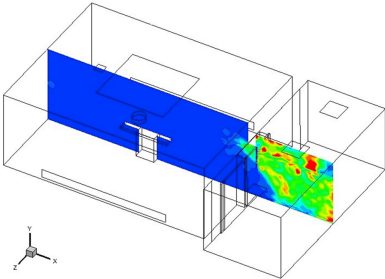


(c) Opening of the door $\Delta Z=1.2\text{m}$, $t=6\text{s}$

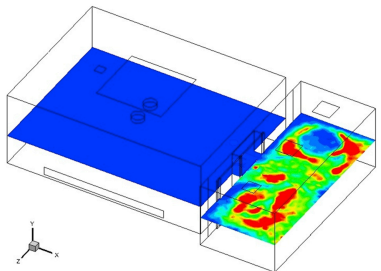
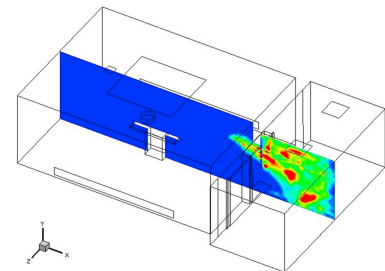


(d) Opening of the door $\Delta Z=1.4\text{m}$, $t=8\text{s}$

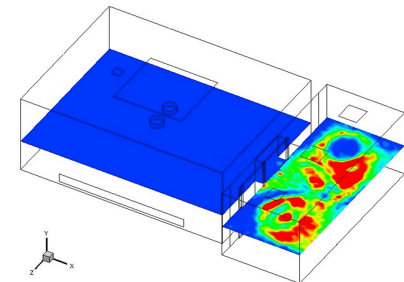
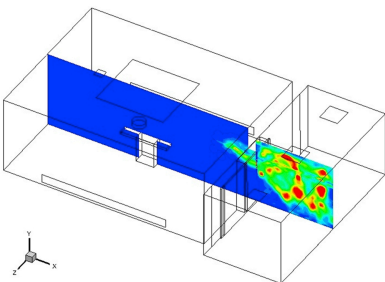




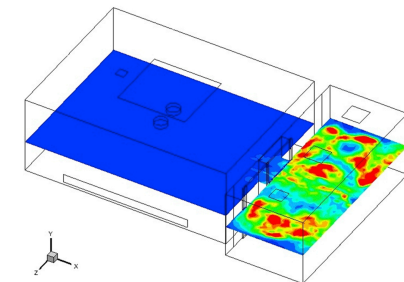
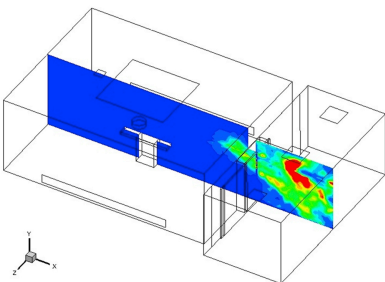
(I) Condition 1-1, $\Delta T=1^{\circ}\text{C}$, $t=11\text{s}$



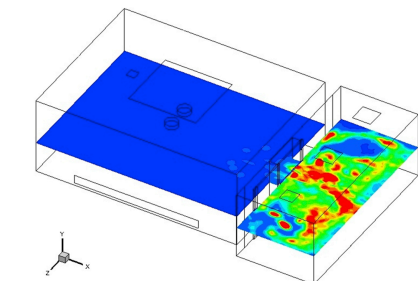
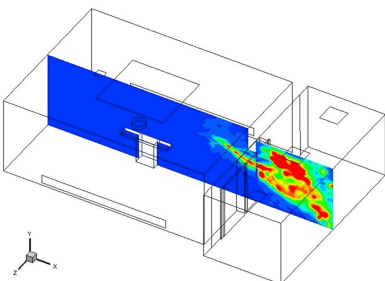
(II) Condition 1-2, $\Delta T=2^{\circ}\text{C}$, $t=11\text{s}$



(III) Condition 1-3, $\Delta T=3^{\circ}\text{C}$, $t=11\text{s}$



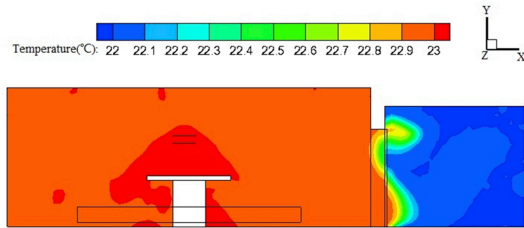
(IV) Condition 1-4, $\Delta T=4^{\circ}\text{C}$, $t=11\text{s}$



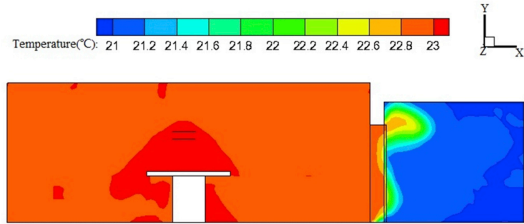
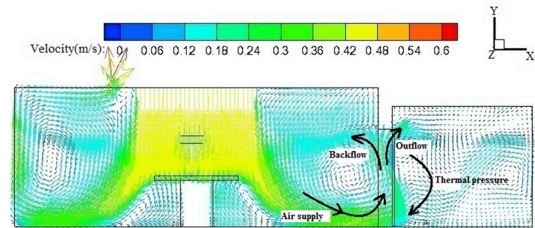
(V) Condition 1-5, $\Delta T=5^{\circ}\text{C}$, $t=11\text{s}$

(a) Particle concentration contour in plane $Z=3.4\text{m}$

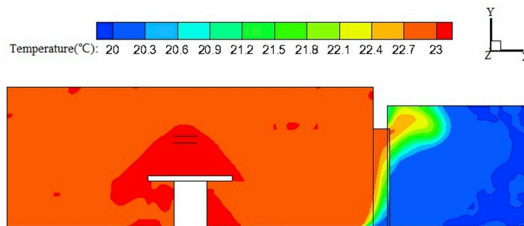
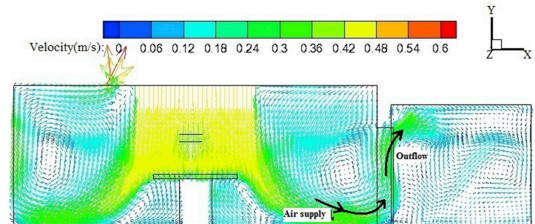
(b) Particle concentration contour in plane $Y=1.2\text{m}$



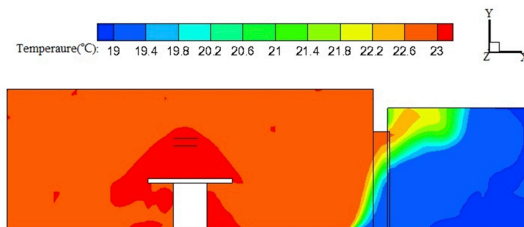
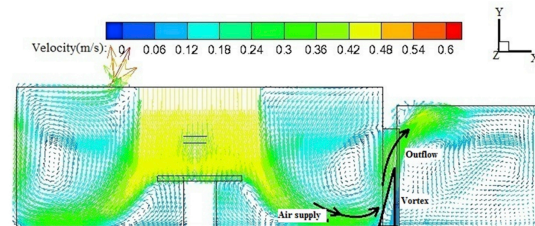
(I) Condition 2-1, $\Delta T=1^\circ\text{C}$, $t=11\text{s}$



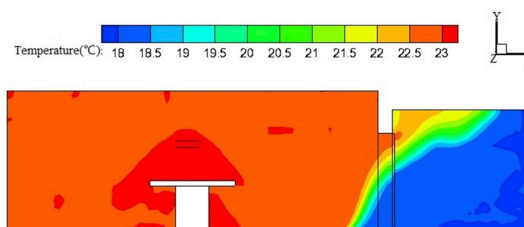
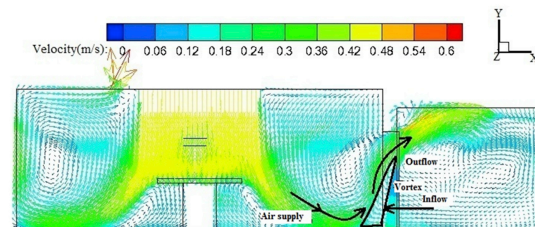
(II) Condition 2-2, $\Delta T=2^\circ\text{C}$, $t=11\text{s}$



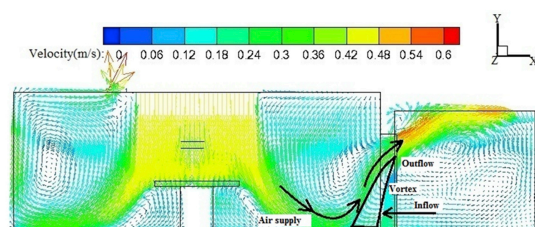
(III) Condition 2-3, $\Delta T=3^\circ\text{C}$, $t=11\text{s}$



(IV) Condition 2-4, $\Delta T=4^\circ\text{C}$, $t=11\text{s}$

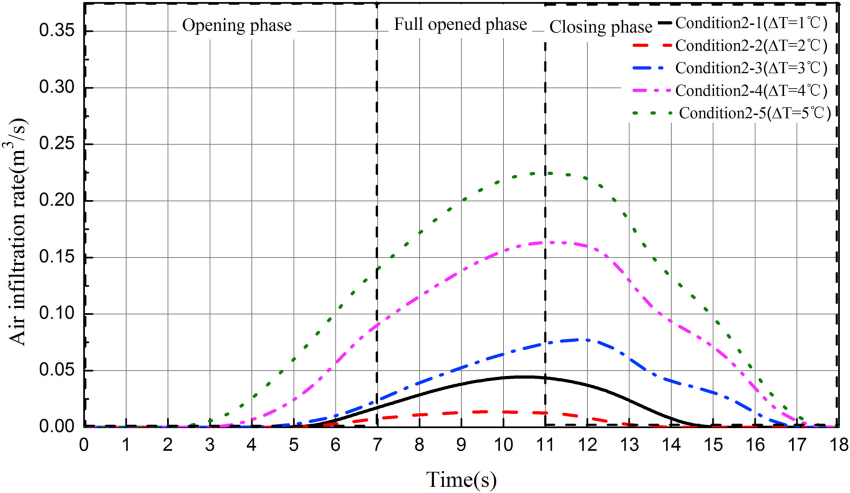


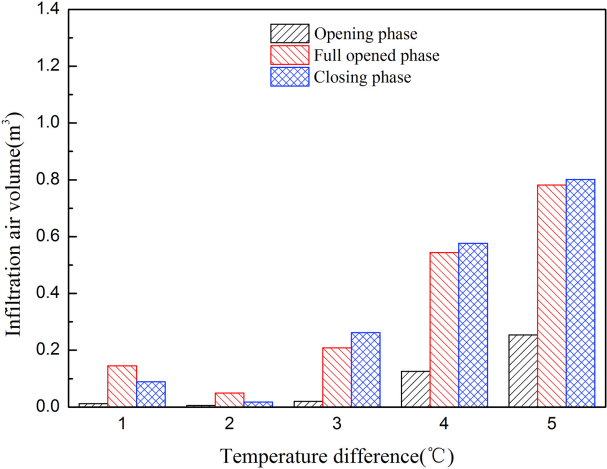
(V) Condition 2-5, $\Delta T=5^\circ\text{C}$, $t=11\text{s}$

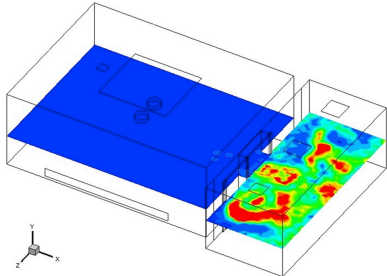
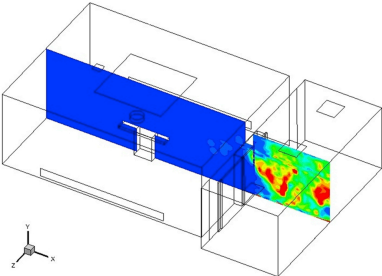


(a) Temperature contour in plane $Z=3.4\text{m}$

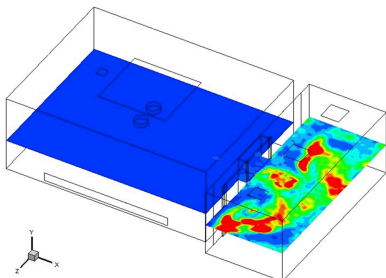
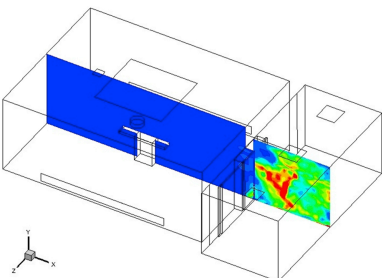
(b) Velocity vector in plane $Z=3.4\text{m}$



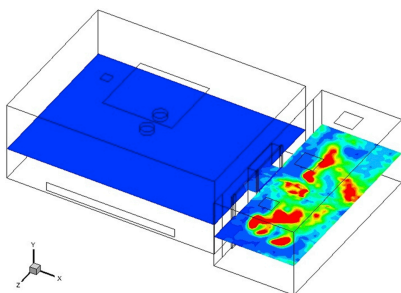
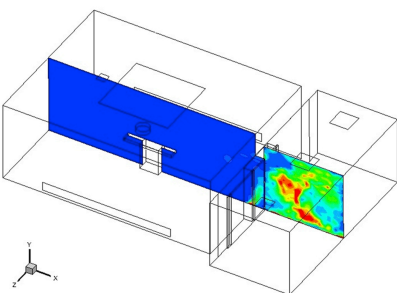




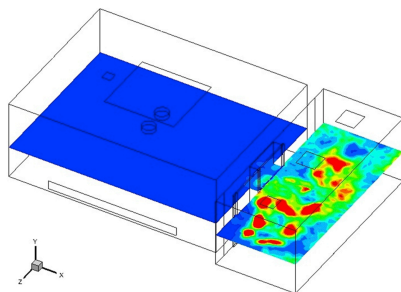
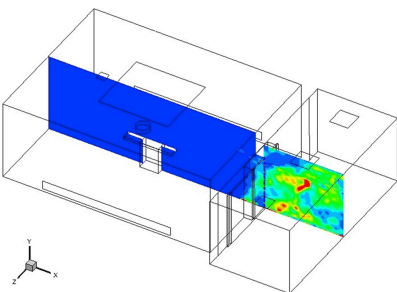
(I) Condition 2-1, $\Delta T=1^\circ\text{C}$, $t=11\text{s}$



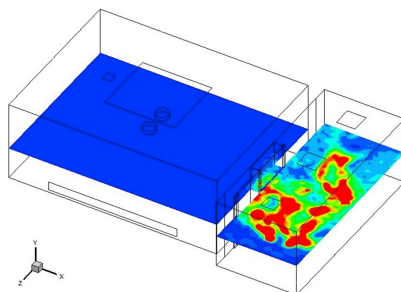
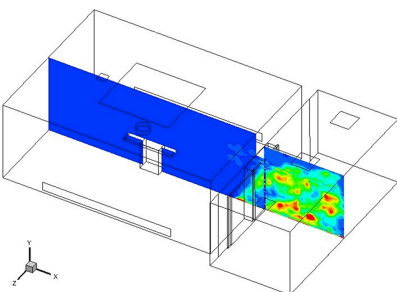
(II) Condition 2-2, $\Delta T=2^\circ\text{C}$, $t=11\text{s}$



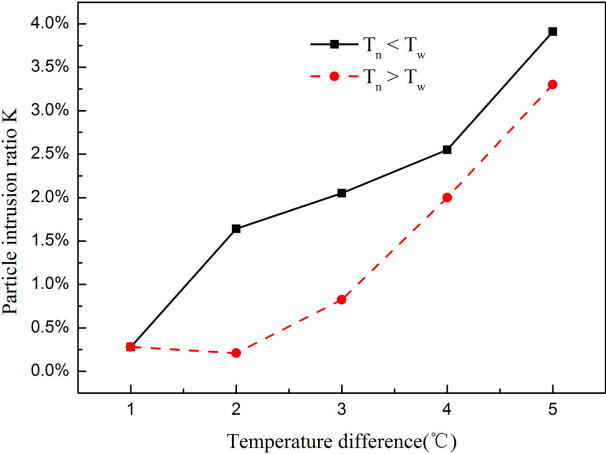
(III) Condition 2-3, $\Delta T=3^\circ\text{C}$, $t=11\text{s}$

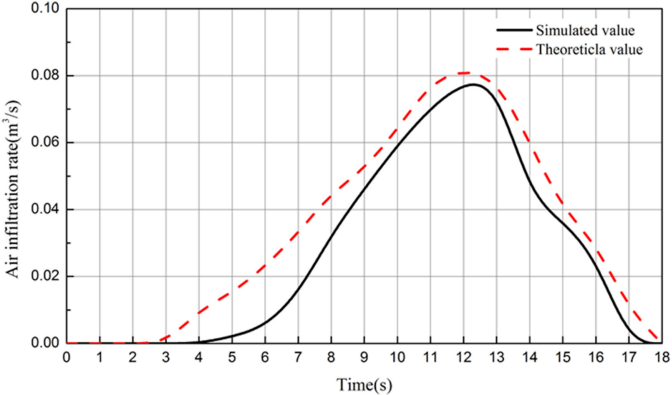


(IV) Condition 2-4, $\Delta T=4^\circ\text{C}$, $t=11\text{s}$

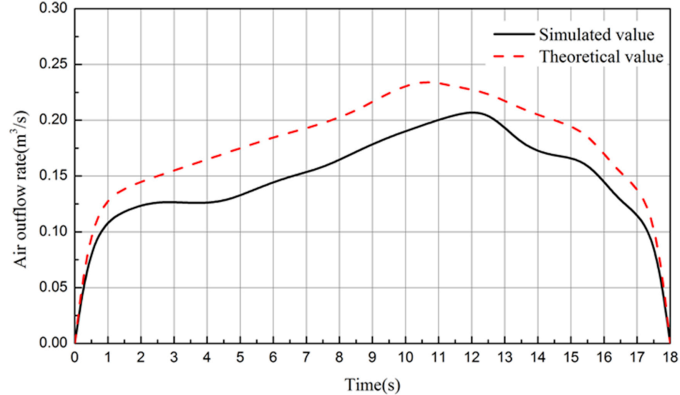


(V) Condition 2-5, $\Delta T=5^\circ\text{C}$, $t=11\text{s}$

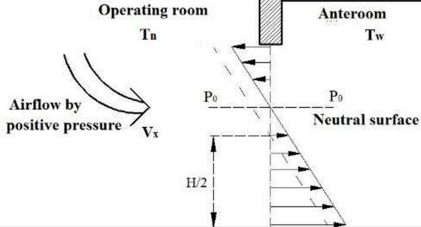




(a) Air infiltration rate into the operating room



(b) Air outflow rate from the operating room



Air exhaust opening
in operating room

Laminar airflow
supply opening

Air supply opening
in anteroom

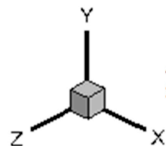
Operating lamps

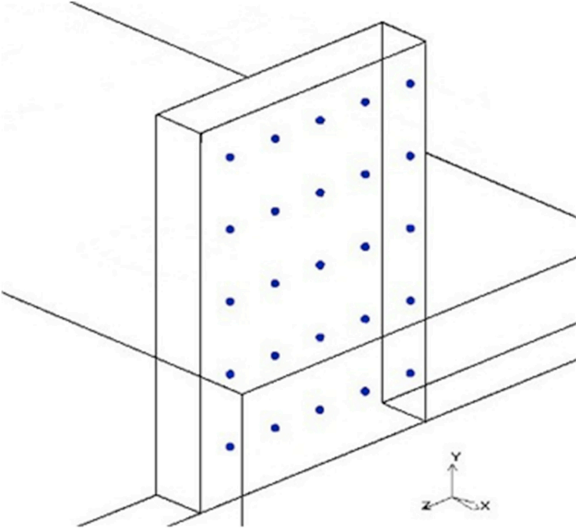
Operating table

Door

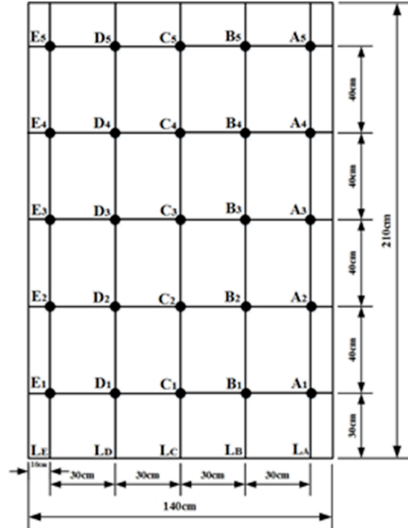
Air return opening
in anteroom

Air return opening
in operating room

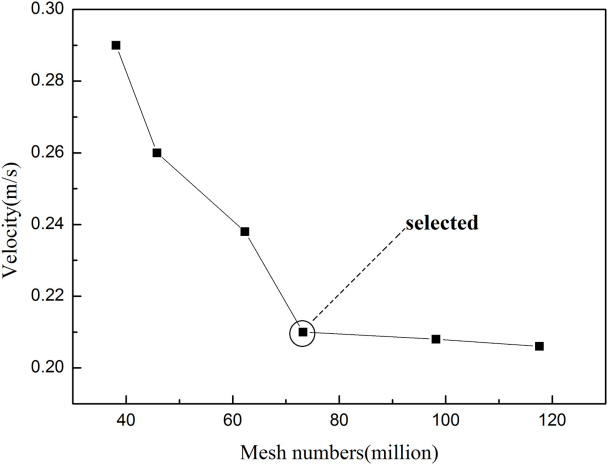


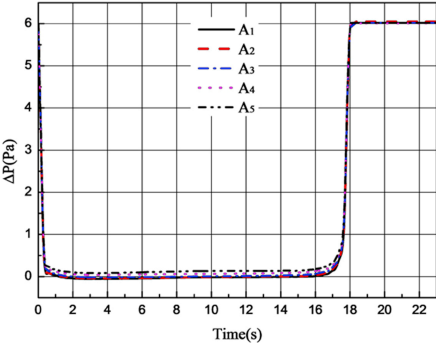


(a) Schematics of monitoring point

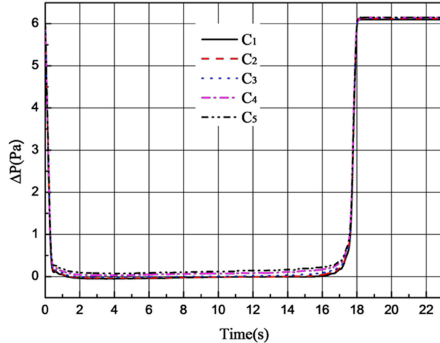


(b) Location of monitoring point

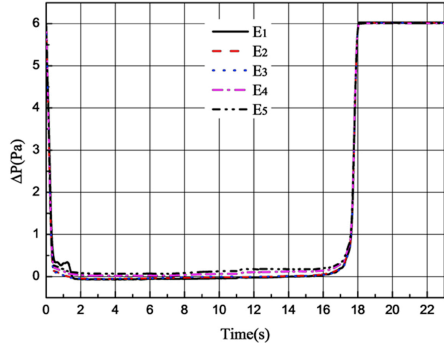




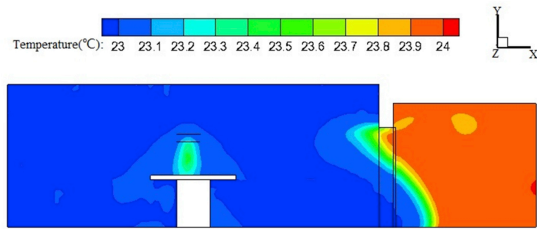
(a) Position A₁ to A₅



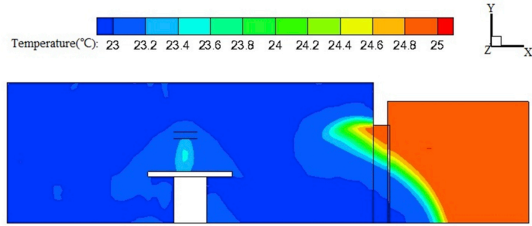
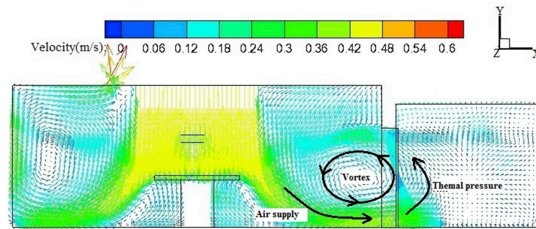
(b) Position C₁ to C₅



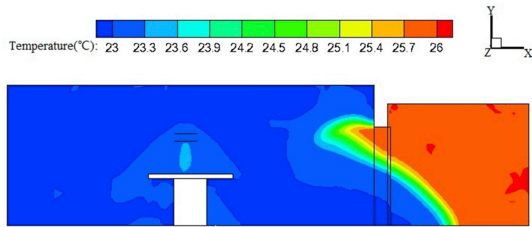
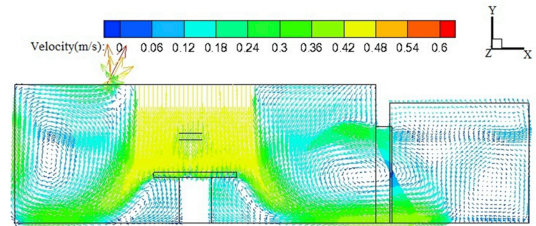
(c) Position E₁ to E₅



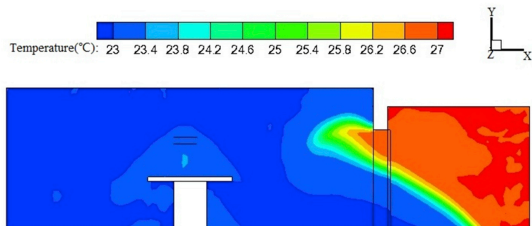
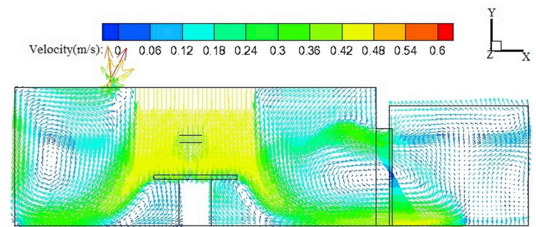
(I) Condition 1-1, $\Delta T=1^\circ\text{C}$, $t=11\text{s}$



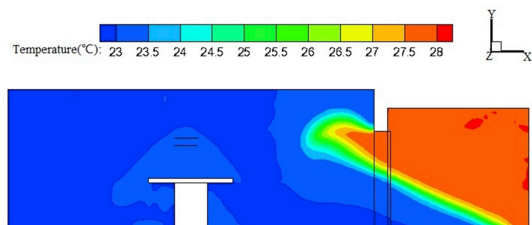
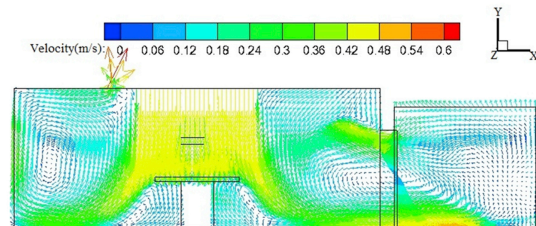
(II) Condition 1-2, $\Delta T=2^\circ\text{C}$, $t=11\text{s}$



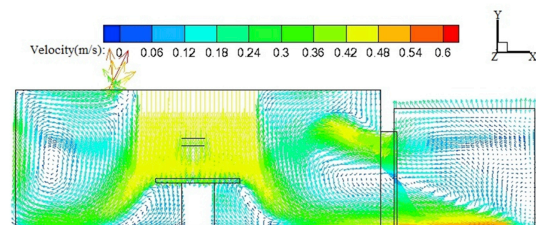
(III) Condition 1-3, $\Delta T=3^\circ\text{C}$, $t=11\text{s}$



(IV) Condition 1-4, $\Delta T=4^\circ\text{C}$, $t=11\text{s}$

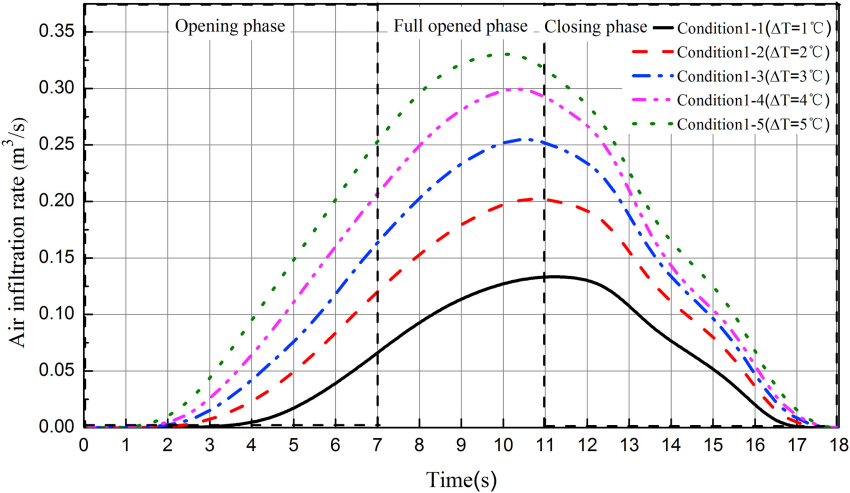


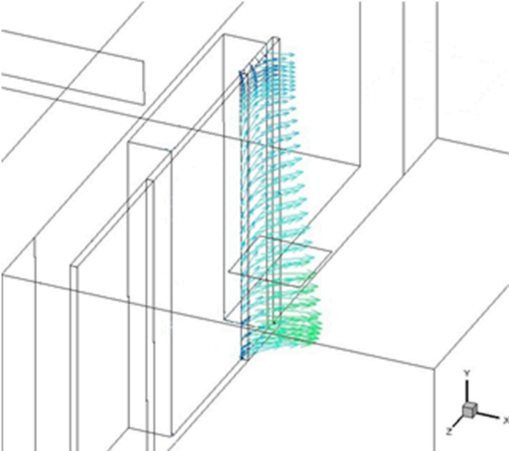
(V) Condition 1-5, $\Delta T=5^\circ\text{C}$, $t=11\text{s}$



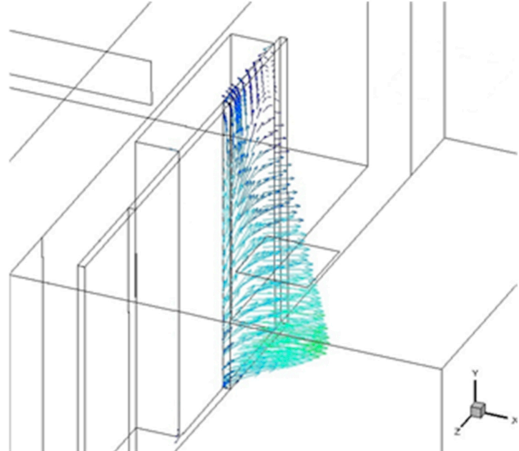
(a) Temperature contour in plane $Z=3.4\text{m}$

(b) Velocity vector in plane $Z=3.4\text{m}$

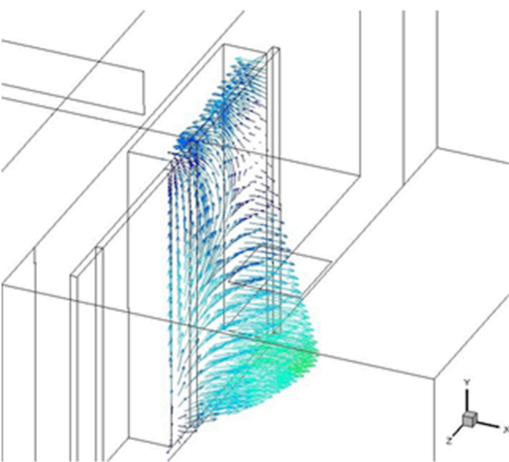




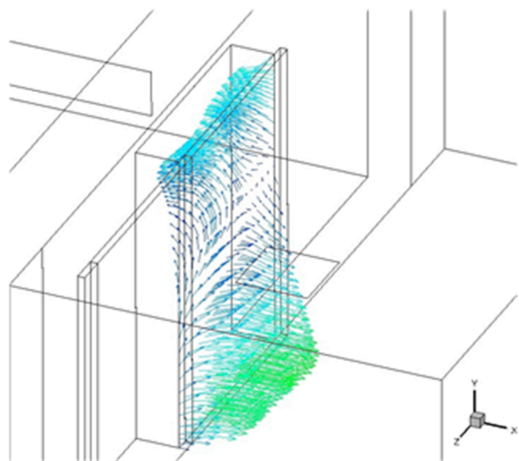
(a) Opening of the door $\Delta Z=0.4\text{m}$, $t=2\text{s}$



(b) Opening of the door $\Delta Z=0.8\text{m}$, $t=4\text{s}$



(c) Opening of the door $\Delta Z=1.2\text{m}$, $t=6\text{s}$



(d) Opening of the door $\Delta Z=1.6\text{m}$, $t=8\text{s}$

Highlights

- Interface airflow of sliding door with temperature/pressure differences is studied.
- Theoretical model was established for interface flow under the coupled effect.
- Air infiltration rate of the closing phase is more than that of the opening phase.